International Journal of Pharmacology

ISSN 1811-7775

science alert

ansinet
Asian Network for Scientific Information

OPEN ACCESS International Journal of Pharmacology

ISSN 1811-7775
DOI: 10.3923/ijp.2018.310.319

Research Article
MicroRNA Microarray Analysis to Investigate the Key Genes and microRNAs Regulated by *Amomum cardamomum* in Nephropathy Rat Model

[1]M.M. Hongmei Chen, [2]M.D. Xiulan Wang, [2]M.M. Enhesuren, [2]B.M. Chang Chun, [2]B.M. Wenjie Jin and [2]B.M. Mengqiqige

[1]Affiliated Hospital of Inner Mongolia University for the Nationalities, 028000 Tongliao, Inner Mongolia Autonomous of China, China
[2]College of Traditional Mongolian Medicine and Pharmacy of Inner Mongolia University for the Nationalities, 028000 Tongliao, Inner Mongolia Autonomous of China, China

Abstract

Background and Objective: Nephropathy is a chronic non-communicable disease that can result in serious consequences. As the dried fruit of Zingiberaceae plant, *Amomum cardamomum* can improve renal function. This study aimed to reveal the action mechanisms of *Amomum cardamomum* in nephropathy rats. **Materials and Methods:** After nephropathy rat model was established, nephropathy rats were divided into model and drug groups (treated with *Amomum cardamomum*). The microRNA (miRNA) expression profilings of the rats were generated and the differentially expressed miRNAs (DE-miRNAs) between control and model groups were analyzed using the limma package. The DE-miRNAs between drug and model groups were also analyzed and then their targets were predicted by the miRWalk2.0 tool. Using DAVID tool, functional enrichment analysis for target genes was performed. In addition, protein-protein interaction (PPI) network and module analyses were conducted for target genes and miRNA-miRNA co-regulatory network was also constructed. **Results:** The nephropathy rat model was successfully established. A total of 21 DE-miRNAs were identified in drug group compared with model group. In the PPI networks, *TP53*, *AKT2*, *HDAC1* and *STAT3* had higher degrees. Besides, *TP53* could interact with *AKT2* and *HDAC1*. Moreover, *STAT3* was co-regulated by *rno-miR-30a-3p* and *rno-miR-30e-5p*. Additionally, functional enrichment analysis showed that *rno-miR-30a-3p*-*rno-miR-30e-5p*, *rno-miR-195-3p*-*rno-miR-32-3p* separately had synergistic effects. **Conclusion:** *Amomum cardamomum* might improve the renal function of nephropathy rats by regulating *TP53*, *AKT2*, *HDAC1*, *STAT3*, *miR-30a-5p*, *miR-30e-5p* and *miR-195-3p*.

Key words: Nephropathy, *Amomum cardamomum*, differentially expressed miRNAs, target genes, miRNA-miRNA co-regulatory network

Received: May 21, 2017 Accepted: November 13, 2017 Published: March 15, 2018

Citation: M.M. Hongmei Chen, M.D. Xiulan Wang, M.M. Enhesuren, B.M. Chang Chun, B.M. Wenjie Jin and B.M. Mengqiqige, 2018. MicroRNA microarray analysis to investigate the key genes and microRNAs regulated by *Amomum cardamomum* in nephropathy rat model. Int. J. Pharmacol., 14: 310-319.

Corresponding Author: Xiulan Wang, College of Traditional Mongolian Medicine and Pharmacy of Inner Mongolia University for the Nationalities, 028000 Tongliao, Inner Mongolia Autonomous of China, China Tel/Fax: +86-0475-8314243

Competing Interest: The authors have declared that no competing interest exists.

Data Availability: All relevant data are within the paper and its supporting information files.

INTRODUCTION

Nephropathy (also named kidney disease or renal disease) is damage to or disease of a kidney. Nephropathy is usually caused by administration of analgesics, deposition of the IgA antibodies in the glomerulus, toxicity of chemotherapy agents and xanthine oxidase deficiency[1]. Nephropathy without effective controlling can result in serious consequences, such as renal insufficiency, renal failure and uremia[2]. Millions of people are undergoing nephropathy globally, among which thousands of people need kidney transplants[3]. Therefore, revealing the key mechanisms underlying nephropathy is of great significance for developing effective therapeutic strategies.

The pathogenesis of nephropathy has been explored by several researches. For example, kidney-targeting *Smad7* gene transfer may improve type 2 diabetic nephropathy through inhibiting the nuclear factor κB (NF-κB) and transforming growth factor-β (TGF-β)/SMAD signaling pathways[4]. The increased matrix metalloproteinase-9 (MMP-9) is adverse in renal interstitial fibrogenesis, which can result in the destruction of tubular basement membrane and the promotion of epithelial to myofibroblast transition[5]. MicroRNA-21 (miR-21) is reported to play an important role in the pathology of fibrosis and is suggested as a target for the treatment of diabetic nephropathy[6,7]. The *miR-135a* functions in renal fibrosis via regulating transient receptor potential cation channel, subfamily C, member 1 (*TRPC1*) and inhibition of *miR-135a* is considered effective for treating diabetic nephropathy[8]. The expression of *miR-29c* in urinary exosome has impacts on both the degree of histological fibrosis and renal function, suggesting that *miR-29c* may serve as a promising marker for renal fibrosis[9,10].

Cardamom (*Amomum cardamomum*) is the dried fruit of *Amomum cardamomum*, which is a perennial herb belonging to the Ginger family and having strong antioxidant activity[11]. *Amomum cardamomum* has been found to improve renal function of alloxan induced diabetic rats and induce the decreased uric acid, creatinine, urea and the enhanced serum protein activity[12]. However, the action mechanisms of *Amomum cardamomum* in nephropathy have not been fully revealed yet.

In this study, Wistar rats were injected with doxorubicin hydrochloride to establish nephropathy rat model. Then, *Amomum cardamomum* was used to treat the rats with nephropathy. The miRNA expression profiling of the rats was then generated, followed by identification of the differentially expressed miRNAs (DE-miRNAs) and prediction of their targets. Subsequently, functional enrichment analysis, protein-protein interaction (PPI) network and module analyses for target genes was performed. Besides, miRNA-miRNA co-regulatory network was also constructed. The objective of this study was to identify the key miRNAs and genes associated with the effects of *Amomum cardamomum* on nephropathy. The findings of this study will help to discover new drug targets for nephropathy, thus improving the clinical outcome of this disease.

MATERIALS AND METHODS

Sample treatment: Male Wistar rats weighting 200-220 g were obtained from Yisi Laboratory Animal Technology Co., Ltd. (Jilin, Changchun, China). After the rats were fed for 5 days, their 24 h urine was collected and then urine protein quantity was determined. A total of 15 rats with normal urine protein quantity were chosen, from which 5 rats were randomly included into normal control group and were injected with normal saline (6.5 mL kg^{-1}) through caudal vein. The remaining 10 rats were injected with doxorubicin hydrochloride (6.5 mg kg^{-1}, Shenzhen Arcandor's Pharmaceutical Co., LTD, Guangdong, Shenzhen, China) into caudal vein to establish nephropathy rat model. From the 4th day after establishment of nephropathy rat model, 5 rats were randomly included into drug group which were treated with *Amomum cardamomum* (3.0 g kg^{-1}, once a day, continuing for 21 days, Tong Kang Pharmaceutical Co., LTD, Hebei, Anguo, China) by intragastric administration, while the other 5 rats were given by gavage with the same volume of distilled water as model group. Meanwhile, the rats in control group were also given by gavage with the same volume of distilled water.

Microarray detection and DE-miRNAs screening: The miRNA expression profilings of the rats were generated by miRNA 4.0 Array (Affymetrix, Santa Clara, CA). Then, the raw data were preprocessed using the Robust Multichip Average (RMA) method of Affy package[13] in R, including background correction and normalization. To confirm whether nephropathy rat model was successfully established or not, the DE-miRNAs between control and model groups were identified using the t-test method[14] in limma package[15]. In addition, the DE-miRNAs between drug group and model group were also analyzed using the same method. The p-value$\leq$0.05 and $|\log_2$ fold change (FC)$|$>0.58 were taken as the thresholds.

Prediction of the targets of DE-miRNAs: Based on the information of miRWalk[16], MicroT4[17], miRanda[18], miRBridge[19], miRDB[20], miRMap[21], miRNAMap[22], PICTAR2[23], PITA[24], RNA22[25], RNAhybrid[26] and TargetScan[27] databases, the genes targeted by the DE-miRNAs between drug group and model group were predicted using the miRWalk2.0 tool[28]. The miRNA-gene pairs predicted by no less than 6 databases were selected.

Functional and pathway enrichment analysis: Gene ontology (GO) database introduces gene products from molecular function (MF), biological process (BP) and cellular component (CC) aspects[29]. The Kyoto Encyclopedia of Genes and Genomes (KEGG) database is developed for predicting the pathways involving genes or other molecules[30]. Using the Database for Annotation, Visualization and Integrated Discovery (DAVID) online tool[31], GO functional and KEGG pathway enrichment analyses for target genes of the DE-miRNAs were performed, with p-value<0.05 and gene count>2 as the thresholds.

PPI network and module analyses: The PPI pairs among the target genes were predicted by the Search Tool for the Retrieval of Interacting Genes (STRING, version10,)[32] database and then PPI network was visualized by Cytoscape software[33]. Using the CytoNCA plug-in (parameter: Without weight)[34] in cytoscape software, closeness centrality (CC), degree centrality (DC) and betweenness centrality (BC) of the nodes in the PPI network were calculated to identify the hub proteins[35]. Using the MCODE plug-in (parameters: Degree cutoff = 2, node score cutoff = 0.2, Max. depth = 100, K-core = 2)[36] in cytoscape software, module analysis was carried out for the PPI network.

Analysis of co-regulated target genes: Based on the target genes co-regulated by two miRNAs, miRNA-miRNA co-regulatory network was constructed by Cytoscape software[33]. For miRNA-miRNA pairs co-regulated more than 10 target genes, their targets were performed with GO functional enrichment analysis, with $p<0.05$ as the threshold. If the target genes co-regulated by two miRNAs were enriched in no less than one GO_BP term, the two miRNAs were thought to have synergistic effects in functional level.

RESULTS

Model validation and DE-miRNAs screening: Under the thresholds of $p \leq 0.05$ and $|\log_2 FC| > 0.58$, a total of 3645 DE-miRNAs in model group compared with control group were screened, including 1324 up and 2321 down-regulated miRNAs, indicating that nephropathy rat model was successfully established. The heat map of clustering analysis was shown in Fig. 1. In addition, a total of 21 DE-miRNAs were identified in drug group compared with model group, including 6 up- and 15 down-regulated miRNAs (Fig. 2). For the up-regulated and down-regulated miRNAs, 906 and 1653 miRNA→target gene pairs were predicted, respectively. The number of genes targeted by each DE-miRNA was listed in Table 1.

Table 1: Number of genes targeted by each differentially expressed miRNA

Category	miRNA	Number of target genes
Up-regulated	*rno-miR-32-3p*	248
	rno-miR-34a-5p	233
	rno-miR-465-5p	216
	rno-miR-195-3p	176
	rno-miR-496-5p	33
Down-regulated	*rno-miR-30e-5p*	333
	rno-miR-30a-3p	288
	rno-miR-665	144
	rno-miR-146a-5p	132
	rno-miR-30c-1-3p	108
	rno-miR-664-1-5p	91
	rno-miR-541-5p	90
	rno-miR-345-5p	89
	rno-miR-345-3p	81
	rno-miR-200a-5p	71
	rno-miR-192-3p	70
	rno-miR-505-5p	58
	rno-miR-504	52
	rno-miR-342-5p	46

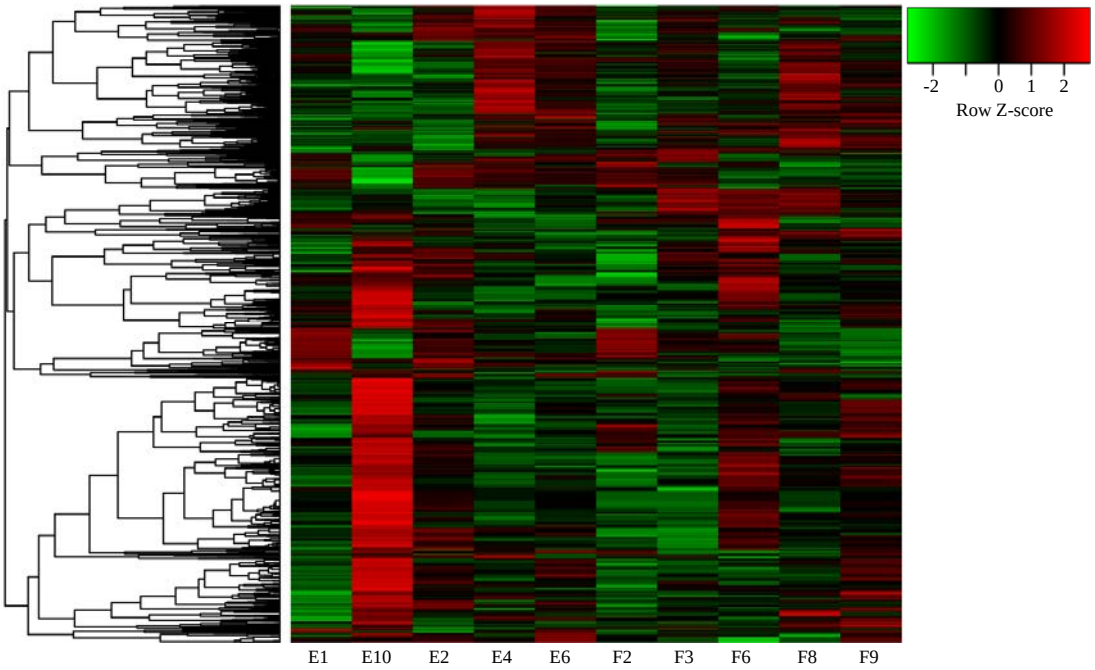

Fig. 1: The heat map of clustering analysis for the differentially expressed miRNAs (DE-miRNAs) between model group and control group

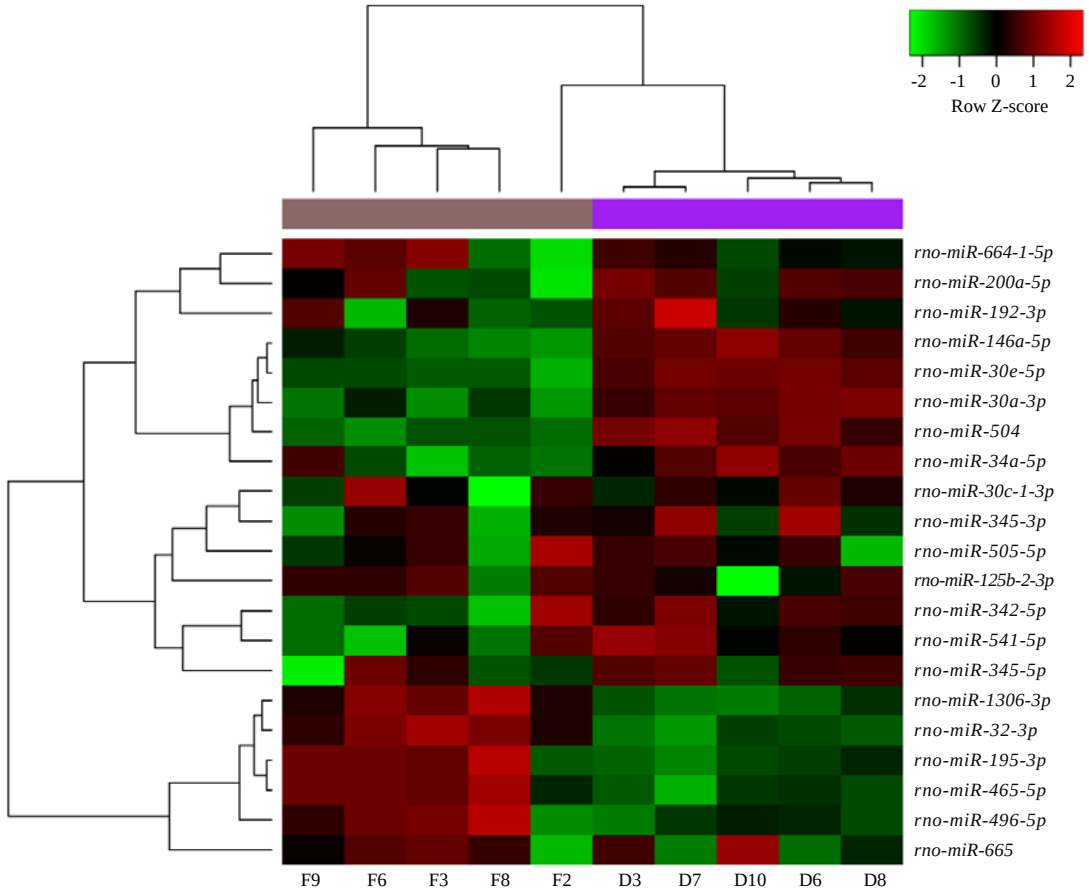

Fig. 2: The heat map of clustering analysis for the differentially expressed miRNAs (DE-miRNAs) between drug group and model group

Functional and pathway enrichment analysis: The GO functional and pathway enrichment analyses for target genes were performed. The target genes of up-regulated miRNAs were mainly enriched in GO_BP function associated with neuron differentiation and cell cycle pathway (KEGG) (Fig. 3a). Meanwhile, the target genes of down-regulated miRNAs were enriched in GO_BP function related to regulation of transcription and pathways in cancer (KEGG) (Fig. 3b).

PPI network and module analyses: The PPI networks for the target genes of up-regulated miRNAs and down-regulated miRNAs were constructed separately. The nodes with higher degrees in the PPI networks were listed in Table 2, including tumor protein p53 (*TP53*, degree = 97), v-akt murine thymoma viral oncogene homolog 2 (*AKT2*, degree = 51) and histone deacetylase 1 (*HDAC1*, degree = 48) targeted by up-regulated miRNAs, as well assignal transducer and activator of transcription 3 (*STAT3*, degree = 71) targeted by down-regulated miRNAs. Importantly, *TP53* had interactions with both *AKT2* and *HDAC1*. The most significant module (score = 10) identified from the PPI network for the target genes of up-regulated miRNAs was shown in Fig. 4a, which

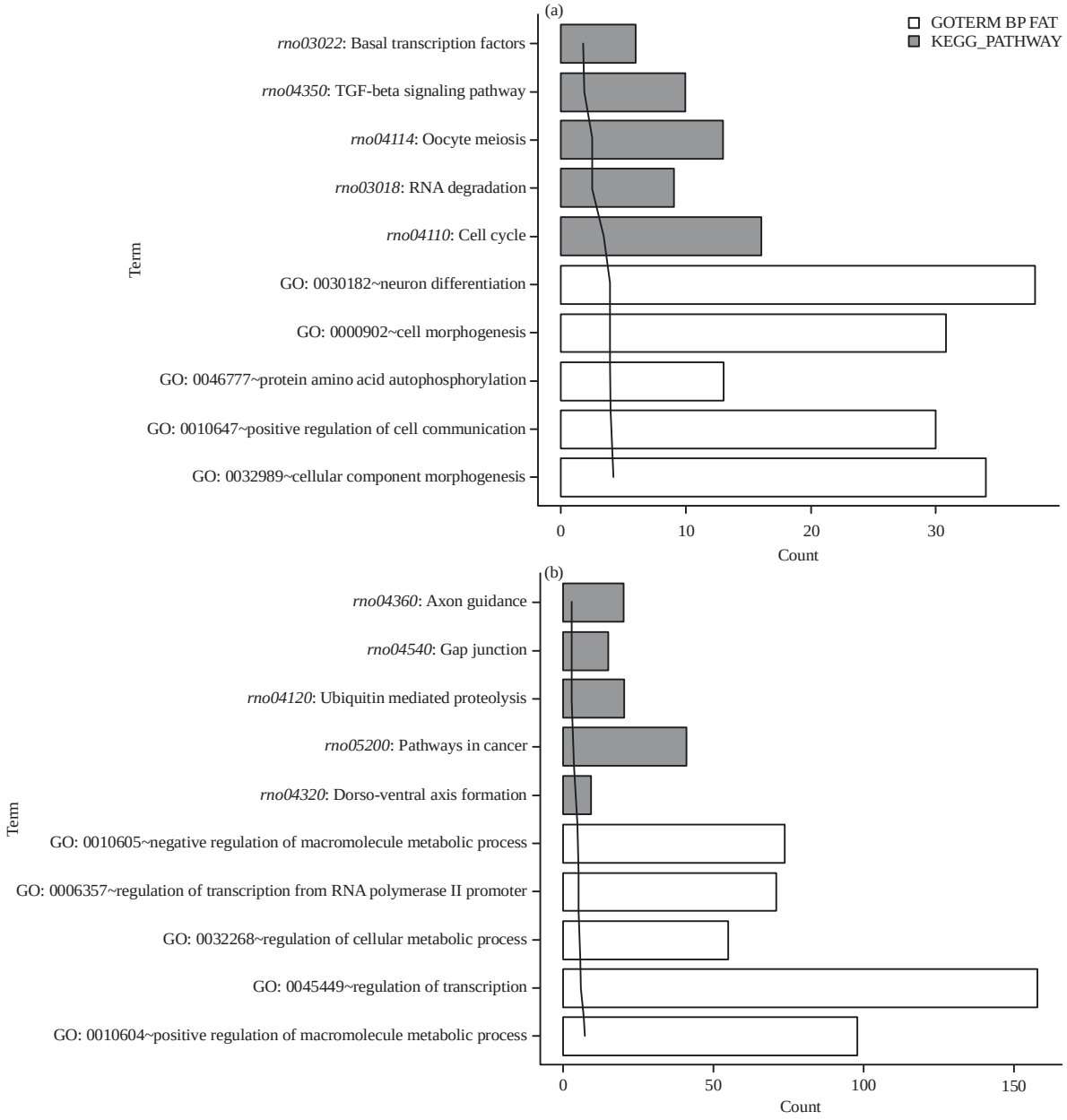

Fig. 3(a-b): The top 5 terms enriched for the target genes of (a) Up-regulated miRNAs and (b) Down-regulated miRNAs
GO: Gene ontology, BP: Biological process, KEGG: Kyoto Encyclopedia of Genes and Genomes

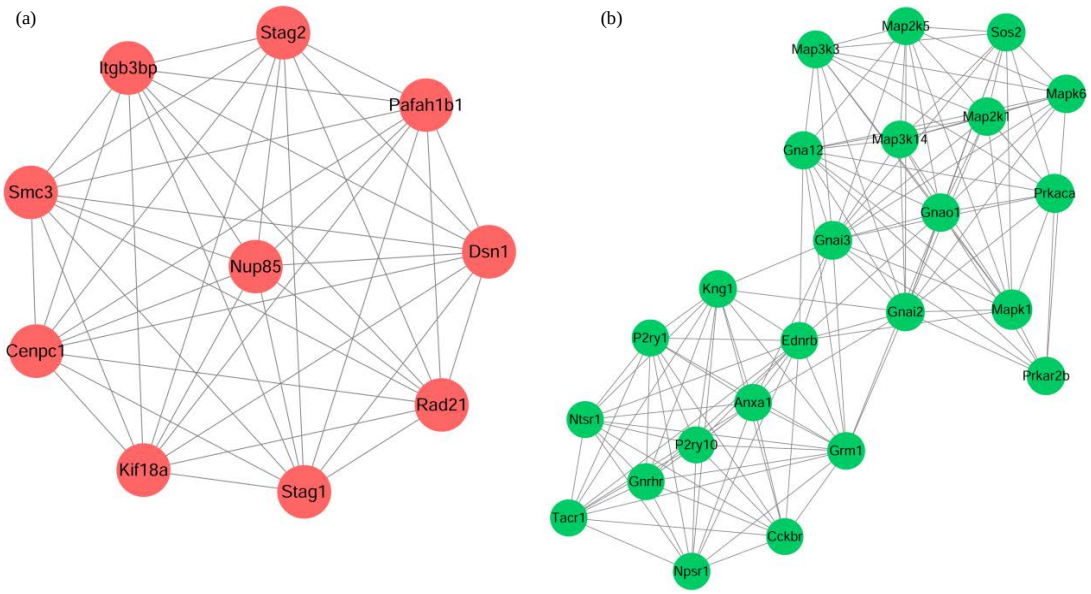

Fig. 4(a-b): The most significant modules identified from the protein-protein interaction (PPI) network for the target genes of (a) Up-regulated miRNAs and (b) Down-regulated miRNAs

Table 2: The nodes with higher degrees in the protein-protein interaction (PPI) networks for the target genes of up-regulated miRNAs and down-regulated miRNAs

Gene	Degree	Betweenness	Closeness	Type
Target genes of up-regulated miRNAs				
Tp53	97.0	99366.055	0.08107448	Up
Akt2	51.0	36810.605	0.079778925	Up
Hdac1	48.0	17889.887	0.07915127	Up
Hdac2	47.0	19877.676	0.07924573	Up
Notch1	42.0	26596.336	0.07928358	Up
Frk	39.0	27861.924	0.079179585	Up
Phlpp1	39.0	13753.14	0.077998355	Up
Prkx	38.0	19557.184	0.07776086	Up
Cdk5	31.0	12090.348	0.07857988	Up
Kdm2a	30.0	9694.378	0.07591174	Up
Kdm2b	30.0	9162.466	0.07581639	Up
Xrn1	30.0	9417.7295	0.075266376	Up
Target genes of down-regulated miRNAs				
Mapk1	100.0	89631.664	0.09520822	Down
Acly	90.0	146575.72	0.09423271	Down
Egfr	76.0	71489.195	0.09447471	Down
Stat3	71.0	55094.82	0.094276614	Down
Notch1	70.0	55520.746	0.093629494	Down
Prkaca	67.0	33364.79	0.092891574	Down
Ubl4a	63.0	84541.445	0.093875654	Down
Jup	63.0	55163.332	0.09384663	Down
Frk	61.0	43305.36	0.09429126	Down
Gnai3	59.0	23465.291	0.09232641	Down
Mapk6	51.0	11093.591	0.09260813	Down
Gnai2	51.0	7956.585	0.091127455	Down
Mapk9	51.0	44580.668	0.093687296	Down
Gnao1	50.0	10491.736	0.09129879	Down

had 10 nodes and 45 edges. Moreover, the most significant module (score = 11.739) of the PPI network constructed for the target genes of down-regulated miRNAs had 24 nodes and 135 edges (Fig. 4b).

Analysis of co-regulated target genes: The miRNA-miRNA co-regulatory network was shown in Fig. 5 and the miRNA-miRNA pairs which co-regulated more than 10 target genes were listed in Table 3. Especially,

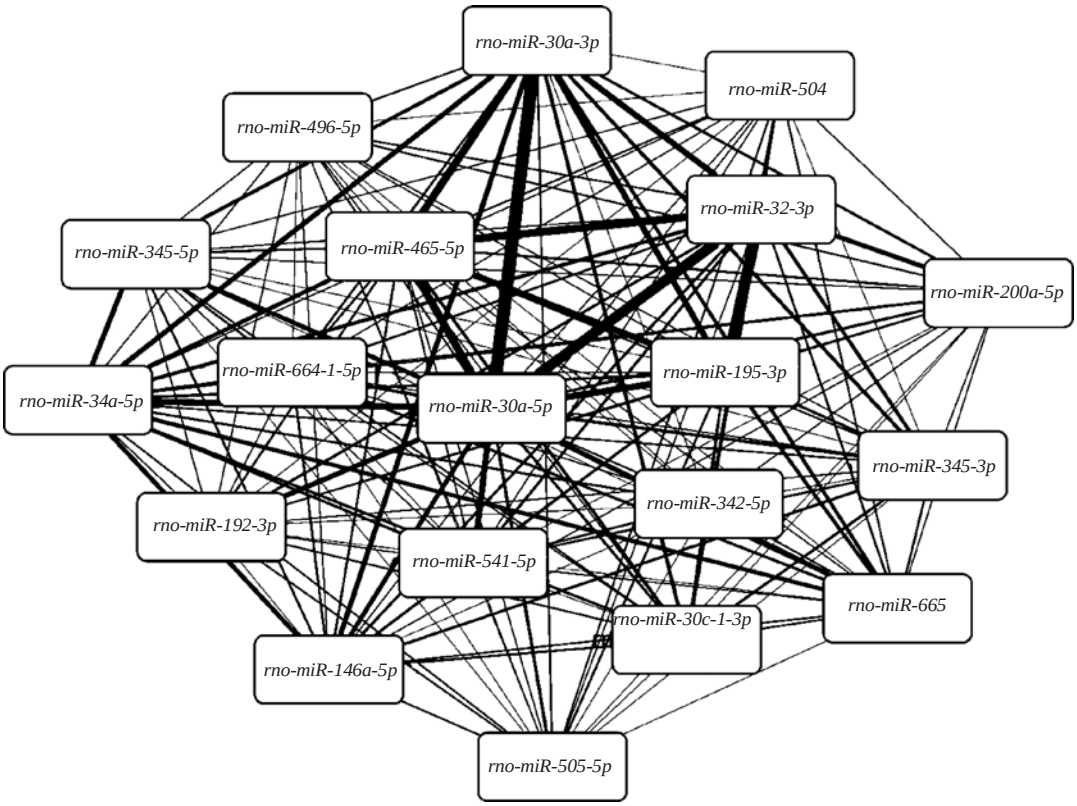

Fig. 5: The miRNA-miRNA co-regulatory network. The thickness of edges represents the number of co-regulated genes

Table 3: The miRNA-miRNA pairs co-regulated more than 10 target genes

mir1	*miR2*	Number
rno-miR-30a-3p	*rno-miR-30e-5p*	26
rno-miR-195-3p	*rno-miR-32-3p*	23
rno-miR-30e-5p	*rno-miR-32-3p*	21
rno-miR-30a-3p	*rno-miR-465-5p*	15
rno-miR-30e-5p	*rno-miR-465-5p*	15
rno-miR-32-3p	*rno-miR-465-5p*	15
rno-miR-34a-5p	*rno-miR-30e-5p*	12
rno-miR-30e-5p	*rno-miR-195-3p*	12
rno-miR-195-3p	*rno-miR-465-5p*	12
rno-miR-30a-3p	*rno-miR-195-3p*	11
rno-miR-30a-3p	*rno-miR-32-3p*	11
rno-miR-30e-5p	*rno-miR-541-5p*	11

STAT3 was co-regulated by *rno-miR-30a-3p* and *rno-miR-30e-5p*. Functional enrichment analysis was performed for the target genes of the miRNA-miRNA pairs which co-regulated more than 10 targets and the number of enriched terms for each miRNA-miRNA pair was listed in Table 4. Notably, *rno-miR-30a-3p-rno-miR-30e-5p*, *rno-miR-195-3p-rno-miR-32-3p*, *rno-miR-30e-5p-rno-miR-32-3p*, *rno-miR-30a-3p-rno-miR-32-3p* and *rno-miR-30e-5p-rno-miR-541-5p* were miRNA-miRNA pairs that had synergistic effects.

DISCUSSION

In this study, a total of 21 DE-miRNAs (including 6 up and 15 down-regulated miRNAs) were identified in drug group compared with model group. Afterwards, 906 and 1653 miRNA→target gene pairs were separately predicted for the up-regulated and down-regulated miRNAs. In the PPI networks constructed for the target genes of DE-miRNAs, *TP53*, *AKT2*, *HDAC1* and *STAT3* had higher degrees.

Table 4: The number of enriched terms for each miRNA-miRNA pair. GO, Gene Ontology; BP, biological process

mir1	*miR2*	co-gene	co-GO-BP
rno-miR-30a-3p	*rno-miR-30e-5p*	26	1
rno-miR-195-3p	*rno-miR-32-3p*	23	3
rno-miR-30e-5p	*rno-miR-32-3p*	21	1
rno-miR-30a-3p	*rno-miR-465-5p*	15	0
rno-miR-30e-5p	*rno-miR-465-5p*	15	0
rno-miR-32-3p	*rno-miR-465-5p*	15	0
rno-miR-34a-5p	*rno-miR-30e-5p*	12	0
rno-miR-30e-5p	*rno-miR-195-3p*	12	0
rno-miR-195-3p	*rno-miR-465-5p*	12	0
rno-miR-30a-3p	*rno-miR-195-3p*	11	0
rno-miR-30a-3p	*rno-miR-32-3p*	11	1
rno-miR-30e-5p	*rno-miR-541-5p*	11	1

HDAC1 and *HDAC2* play critical roles in mediating the proliferation of renal interstitial fibroblasts, activation of *STAT3* and expression of cell cycle proteins, additionally, *STAT3* regulates the proliferative effects of HDACs[37]. Trichostatin A (TSA, an HDAC inhibitor) and other HDAC inhibitors are reported to be novel therapeutic agents for tubular epithelial-mesenchymal transition (EMT) in renal epithelial cells[38]. Ursolic acid (UA) has anti-oxidant activity and regulates the NF-κB and *STAT3* signaling pathways, thus it can suppress carbon tetrachloride-induced inflammation in mouse kidney[39]. HIV-1 Nef causes the proliferation and dedifferentiation of podocytes through activating the mitogen-activated protein kinase 1, 2 (*MAPK1,2*) and *STAT3* pathways and *STAT3* functions in the progression of human immunodeficiency virus (HIV)-associated nephropathy[40]. These findings suggest that *HDAC1* and *STAT3* may be involved in the progression of nephropathy.

Through the *p53* activation and *STAT3* dephosphorylation, aristolochic acid (AA) leads to the death of tubular epithelial cells, suggesting that *p53* contributes to renal injury in acute AA nephropathy[41]. The expression levels of *p53*, *TGF-β* and *miR-192* are significantly up-regulated in the rats with diabetic nephropathy, which may accelerate the progression of diabetic nephropathy[42]. *AKT2* acts in preserving podocyte viability and function, indicating that *AKT2* may be used for maintaining glomerular function in chronic kidney disease[43]. Knockdown of *AKT2* antagonizes TGF-β1-induced EMT via suppressing glycogen synthase kinase-3β (GSK3β)/Snail signaling pathway in renal tubular epithelial cells[44]. What's more, *AKT2*/protein kinase B β (*PKBβ*) is reported to function in the regulation of renal phosphate and glucose transports[45,46]. Therefore, *TP53* and *AKT2* may play roles in the pathogenesis of nephropathy. In the PPI network for the target genes of up-regulated miRNAs, TP53 had interactions with both AKT2 and HDAC1, indicating that *TP53* might also function in nephropathy through interacting with *AKT2* and *HDAC1*.

Furthermore, a previous study reveals that the levels of *miR-30a-5p*, *miR-196a* and *miR-490* have correlations with the activity of focal segmental glomerulosclerosis disease[47]. Inhibition of *miR-30a-3p* and *miR-30c-2-3p* promotes hypoxia-inducible factor 2α (*HIF2α*) expression, which reduces the tumor suppressive effects of *HIF1α* in von-Hippel Lindau (VHL)-deficient clear cell renal cell carcinomas (ccRCC)[48]. The miR-30e/uncoupling protein 2 (UCP2) axis is critical for regulating EMT and kidney fibrosis induced by *TGF-β1* and may be a promising therapeutic approach for fibrotic kidney disease[49]. The decreased expression of *miR-195* protects mesangial cells against apoptosis, thus the anti-apoptosis effect of miR-195 may be important for the early stages of diabetic nephropathy[50]. Thus, *miR-30a-5p*, *miR-30e-5p* and *miR-195-3p* may also affect nephropathy. In this study, functional enrichment analysis showed that *rno-miR-30a-3p* and *rno-miR-30e-5p* had synergistic effect. Besides, *STAT3* was co-regulated by *miR-30a-3p* and *miR-30e-5p*. Thus, we speculate that *miR-30a-3p* and *miR-30e-5p* may have a synergistic effect in nephropathy by regulating *STAT3*.

CONCLUSION

It is concluded that *Amomum cardamomum* may improve the renal function of nephropathy rats by regulating several key genes (including *TP53*, *AKT2*, *HDAC1*, *STAT3*, *miR-30a-5p*, *miR-30e-5p* and *miR-195-3p*). However, further experimental researches are still necessary for confirming these findings.

SIGNIFICANCE STATEMENT

This study discovers the synergistic effects of key genes and miRNAs regulated by *Amomum cardamomum* that can be beneficial for improving the renal function of nephropathy rats. This study will help the researcher to uncover the action mechanisms of *Amomum cardamomum* in nephropathy that

many researchers are not able to explore. Thus, a new theory on these gene-miRNA interactions may be arrived at.

ACKNOWLEDGMENTS

This study was supported by Natural Science Foundation of Inner Mongolia Autonomous Region (No. 2012ZD12).

REFERENCES

1. Hajivandi, A. and M. Amiri, 2014. World kidney day 2014: Kidney disease and elderly. J. Parathyroid Dis., 2: 3-4.
2. Lemley, K.V., 2016. Glomerular pathology and the progression of chronic kidney disease. Am. J. Physiol.-Renal Physiol., 310: F1385-F1388.
3. Jha, V., G. Garcia-Garcia, K. Iseki, Z. Li and S. Naicker *et al*., 2013. Chronic kidney disease: Global dimension and perspectives. Lancet, 382: 260-272.
4. Ka, S.M., Y.C. Yeh, X.R. Huang, T.K. Chao and Y.J. Hung *et al*., 2012. Kidney-targeting *Smad7* gene transfer inhibits renal TGF-β/MAD homologue (SMAD) and Nuclear Factor κB (NF-κB) signalling pathways and improves diabetic nephropathy in mice. Diabetologia, 55: 509-519.
5. Wang, X., Y. Zhou, R. Tan, M. Xiong and W. He *et al*., 2010. Mice lacking the matrix metalloproteinase-9 gene reduce renal interstitial fibrosis in obstructive nephropathy. Am. J. Physiol.-Renal Physiol., 299: F973-F982.
6. Zhong, X., A.C.K. Chung, H.Y. Chen, Y. Dong and X.M. Meng *et al*., 2013. miR-21 is a key therapeutic target for renal injury in a mouse model of type 2 diabetes. Diabetologia, 56: 663-674.
7. Wang, J., Y. Gao, M. Ma, M. Li and D. Zou *et al*., 2013. Effect of miR-21 on renal fibrosis by regulating MMP-9 and TIMP1 in kk-ay diabetic nephropathy mice. Cell Biochem. Biophys., 67: 537-546.
8. He, F., F. Peng, X. Xia, C. Zhao and Q. Luo *et al*., 2014. MiR-135a promotes renal fibrosis in diabetic nephropathy by regulating TRPC1. Diabetologia, 57: 1726-1736.
9. Lv, L.L., Y.H. Cao, H.F. Ni, M. Xu and D. Liu *et al*., 2013. MicroRNA-29c in urinary exosome/microvesicle as a biomarker of renal fibrosis. Am. J. Physiol.-Renal Physiol., 305: F1220-F1227.
10. Fang, Y., X. Yu, Y. Liu, A.J. Kriegel and Y. Heng *et al*., 2013. miR-29c is downregulated in renal interstitial fibrosis in humans and rats and restored by HIF-α activation. Am. J. Physiol.-Renal Physiol., 304: F1274-F1282.
11. Charles, D.J., 2012. Cardamom. In: Antioxidant Properties of Spices, Herbs and other Sources, Charles, D.J. (Ed.). Springer, New York, UA., ISBN-13: 978-1-4614-4309-4, pp: 207-212.
12. Verma, D., R. Yadav and M. Kumar, 2015. Effect of seed extract of *Amomum cardamomum* on renal function in alloxan induced diabetic rats. World J. Clin. Pharmacol. Microbiol. Toxicol., 1: 52-54.
13. Gautier, L., L. Cope, B.M. Bolstad and R.A. Irizarry, 2004. Affy-analysis of *Affymetrix GeneChip* data at the probe level. Bioinformatics, 20: 307-315.
14. Smyth, G.K., 2005. Limma: Linear Models for Microarray Data. In: Bioinformatics and Computational Biology Solutions Using R and Bioconductor, Gentleman, R., V.J. Carey, W. Huber, R.A. Irizarry and S. Dudoit (Eds.). Springer, New York, USA., ISBN-13: 978-0-387-25146-2, pp: 397-420.
15. Ritchie, M.E., B. Phipson, D. Wu, Y. Hu, C.W. Law, W. Shi and G.K. Smyth, 2015. *Limma* powers differential expression analyses for RNA-sequencing and microarray studies. Nucleic Acids Res., Vol. 43, No. 7. 10.1093/nar/gkv007.
16. Dweep, H., N. Gretz and C. Sticht, 2014. miRWalk database for miRNA-target interactions. Methods Mol. Biol., 1182: 289-305.
17. Maragkakis, M., T. Vergoulis, P. Alexiou, M. Reczko and K. Plomaritou *et al*., 2011. DIANA-microT Web server upgrade supports Fly and Worm miRNA target prediction and bibliographic miRNA to disease association. Nucleic Acids Res., 39: W145-W148.
18. Enright, A.J., B. John, U. Gaul, T. Tuschl, C. Sander and D.S. Marks, 2003. MicroRNA targets in *Drosophila*. Genome Biol., Vol. 5. 10.1186/gb-2003-5-1-r1.
19. Tsang, J.S., M.S. Ebert and A. van Oudenaarden, 2010. Genome-wide dissection of MicroRNA functions and cotargeting networks using gene set signatures. Mol. Cell, 38: 140-153.
20. Wong, N. and X. Wang, 2014. miRDB: An online resource for microRNA target prediction and functional annotations. Nucleic Acids Res., 43: D146-D152.
21. Vejnar, C.E. and E.M. Zdobnov, 2012. MiRmap: Comprehensive prediction of microRNA target repression strength. Nucleic Acids Res., 40: 11673-11683.
22. Hsu, S.D., C.H. Chu, A.P. Tsou, S.J. Chen and H.C. Chen *et al*., 2007. miRNAMap 2.0: Genomic maps of microRNAs in metazoan genomes. Nucleic Acids Res., 36: D165-D169.
23. Blin, K., C. Dieterich, R. Wurmus, N. Rajewsky, M. Landthaler and A. Akalin, 2014. DoRiNA 2.0-upgrading the doRiNA database of RNA interactions in post-transcriptional regulation. Nucleic Acids Res., 43: D160-D167.
24. Kertesz, M., N. Iovino, U. Unnerstall, U. Gaul and E. Segal, 2007. The role of site accessibility in microRNA target recognition. Nat. Genet., 39: 1278-1284.
25. Miranda, K.C., T. Huynh, Y. Tay, Y.S. Ang and W.L.Tam *et al*., 2006. A pattern-based method for the identification of microrna binding sites and their corresponding heteroduplexes. Cell, 126: 1203-1217.

26. Kruger, J. and M. Rehmsmeier, 2006. RNAhybrid: microRNA target prediction easy, fast and flexible. Nucleic Acids Res., 34: W451-W454.
27. Shin, C., J.W. Nam, K.K.H. Farh, H.R. Chiang, A. Shkumatava and D.P. Bartel, 2010. Expanding the microRNA targeting code: Functional sites with centered pairing. Mol. Cell, 38: 789-802.
28. Dweep, H. and N. Gretz, 2015. miRWalk2.0: A comprehensive atlas of microRNA-target interactions. Nat. Methods, 12: 697-697.
29. Tweedie, S., M. Ashburner, K. Falls, P. Leyland and P. McQuilton *et al*., 2008. FlyBase: Enhancing *Drosophila* gene ontology annotations. Nucleic Acids Res., 37: D555-D559.
30. Kanehisa, M. and S. Goto, 2000. KEGG: Kyoto encyclopedia of genes and genomes. Nucl. Acids Res., 28: 27-30.
31. Dennis, Jr. G., B.T. Sherman, D.A. Hosack, J. Yang, W. Gao, H.C. Lane and R.A. Lempicki, 2003. DAVID: Database for annotation, visualization and integrated discovery. Genome Biol., Vol. 4. 10.1186/gb-2003-4-9-r60.
32. Szklarczyk, D., A. Franceschini, S. Wyder, K. Forslund and D. Heller *et al*., 2014. STRING v10: Protein-protein interaction networks, integrated over the tree of life. Nucl. Acids Res., 43: D447-D452.
33. Saito, R., M.E. Smoot, K. Ono, J. Ruscheinski and P.L. Wang *et al*., 2012. A travel guide to Cytoscape plugins. Nat. Methods, 9: 1069-1076.
34. Tang, Y., M. Li, J. Wang, Y. Pan and F.X. Wu, 2015. CytoNCA: A cytoscape plugin for centrality analysis and evaluation of protein interaction networks. Biosystems, 127: 67-72.
35. He, X. and J. Zhang, 2006. Why do hubs tend to be essential in protein networks? PLoS Genet., Vol. 2. 10.1371/journal.pgen.0020088.
36. Bader, G.D. and C.W. Hogue, 2003. An automated method for finding molecular complexes in large protein interaction networks. BMC Bioinform., Vol. 4. 10.1186/1471-2105-4-2.
37. Pang, M., L. Ma, N. Liu, M. Ponnusamy, T.C. Zhao, H. Yan and S. Zhuang, 2011. Histone deacetylase 1/2 mediates proliferation of renal interstitial fibroblasts and expression of cell cycle proteins. J. Cell. Biochem., 112: 2138-2148.
38. Yoshikawa, M., K. Hishikawa, T. Marumo and T. Fujita, 2007. Inhibition of histone deacetylase activity suppresses epithelial-to-mesenchymal transition induced by TGF-β1 in human renal epithelial cells. J. Am. Soc. Nephrol., 18: 58-65.
39. Ma, J.Q., J. Ding, Z.H. Xiao and C.M. Liu, 2014. Ursolic acid ameliorates carbon tetrachloride-induced oxidative DNA damage and inflammation in mouse kidney by inhibiting the *STAT3* and NF-κB activities. Int. Immunopharmacol., 21: 389-395.
40. Feng, X., T.C. Lu, P.Y. Chuang, W. Fang and K. Ratnam *et al*., 2009. Reduction of *STAT3* activity attenuates HIV-induced kidney injury. J. Am. Soc. Nephrol., 20: 2138-2146.
41. Zhou, L., P. Fu, X.R. Huang, F. Liu, K.N. Lai and H.Y. Lan, 2010. Activation of p53 promotes renal injury in acute aristolochic acid nephropathy. J. Am. Soc. Nephrol., 21: 31-41.
42. Deshpande, S.D., S. Putta, M. Wang, J.Y. Lai and M. Bitzer *et al*., 2013. Transforming growth factor-β-induced cross talk between p53 and a microRNA in the pathogenesis of diabetic nephropathy. Diabetes, 62: 3151-3162.
43. Canaud, G., F. Bienaime, A. Viau, C. Treins and W. Baron *et al*., 2013. AKT2 is essential to maintain podocyte viability and function during chronic kidney disease. Nat. Med., 19: 1288-1296.
44. Lan, A., Y. Qi and J. Du, 2014. Akt2 mediates TGF-β1-induced epithelial to mesenchymal transition by deactivating GSK3β/snail signaling pathway in renal tubular epithelial cells. Cell. Physiol. Biochem., 34: 368-382.
45. Kempe, D.S., G. Siraskar, H. Frohlich, A.T. Umbach and M. Stubs *et al*., 2010. Regulation of renal tubular glucose reabsorption by Akt2/PKBβ. Am. J. Physiol.-Renal Physiol., 298: F1113-F1117.
46. Kempe, D.S., T.F. Ackermann, K.M. Boini, F. Klaus and A.T. Umbach *et al*., 2010. Akt2/PKBβ-sensitive regulation of renal phosphate transport. Acta Physiol., 200: 75-85.
47. Zhang, W., C. Zhang, H. Chen, L. Li and Y. Tu *et al*., 2014. Evaluation of microRNAs *miR-196a*, *miR-30a-5P* and *miR-490* as biomarkers of disease activity among patients with FSGS. Clin. J. Am. Soc. Nephrol., 9: 1545-1552.
48. Mathew, L.K., S.S. Lee, N. Skuli, S. Rao and B. Keith *et al*., 2013. Restricted expression of *miR-30c-2-3p* and *miR-30a-3p* in clear cell renal carcinomas enhances HIF2α activity. Cancer Discov., 4: 53-60.
49. Jiang, L., W. Qiu, Y. Zhou, P. Wen and L. Fang *et al*., 2013. A microRNA-30e/mitochondrial uncoupling protein 2 axis mediates TGF-β1-induced tubular epithelial cell extracellular matrix production and kidney fibrosis. Kidney Int., 84: 285-296.
50. Chen, Y.Q., X.X. Wang, X.M. Yao, D.L. Zhang, X.F. Yang, S.F. Tian and N.S. Wang, 2012. Abated microRNA-195 expression protected mesangial cells from apoptosis in early diabetic renal injury in mice. J. Nephrol., 25: 566-576.